

YALE PEABODY MUSEUM

P.O. BOX 208118 | NEW HAVEN CT 06520-8118 USA | PEABODY.YALE. EDU

JOURNAL OF MARINE RESEARCH

The *Journal of Marine Research*, one of the oldest journals in American marine science, published important peer-reviewed original research on a broad array of topics in physical, biological, and chemical oceanography vital to the academic oceanographic community in the long and rich tradition of the Sears Foundation for Marine Research at Yale University.

An archive of all issues from 1937 to 2021 (Volume 1–79) are available through EliScholar, a digital platform for scholarly publishing provided by Yale University Library at <https://elischolar.library.yale.edu/>.

Requests for permission to clear rights for use of this content should be directed to the authors, their estates, or other representatives. The *Journal of Marine Research* has no contact information beyond the affiliations listed in the published articles. We ask that you provide attribution to the *Journal of Marine Research*.

Yale University provides access to these materials for educational and research purposes only. Copyright or other proprietary rights to content contained in this document may be held by individuals or entities other than, or in addition to, Yale University. You are solely responsible for determining the ownership of the copyright, and for obtaining permission for your intended use. Yale University makes no warranty that your distribution, reproduction, or other use of these materials will not infringe the rights of third parties.



This work is licensed under a Creative Commons Attribution-NonCommercial-ShareAlike 4.0 International License.
<https://creativecommons.org/licenses/by-nc-sa/4.0/>



Internal tidal bores in the nearshore: Warm-water fronts, seaward gravity currents and the onshore transport of neustonic larvae

by **Jesus Pineda**^{1,2}

ABSTRACT

Nearshore temperature fluctuations are associated with energetic cross-shore two-way flows that influence the onshore transport of neustonic larvae. Water temperature near the surface and bottom at two nearshore stations off southern California (6 and 15 m water depth, respectively) can drop sharply and subsequently rise. Two or more consecutive drops and rises can occur at diurnal or semidiurnal periodicities. The temperature increases may be accompanied by energetic seaward bottom currents together with sharp-edged warm-water fronts. (Warm-water fronts are defined here as linear seasurface features dividing parcels of water of different temperature.) Shoreward-moving surface fronts divided bodies of water of different surface temperature, where the coldest water body was inshore. Fronts disappeared at (or close to) the surf zone. The sharp drops in water temperature are interpreted as the onshore advection of subsurface water by large internal tidal bores, and it is concluded that the sudden increases in temperature and cross-shore advection are epiphenomena of internal tidal bores.

Internal tidal bores have been invoked previously to explain the onshore transport of water-column larvae. This study tests the hypothesis that shoreward surface flow, an epiphenomenon of internal tidal bores, transports neustonic larvae in warm-water fronts. Five warm-water fronts were sampled in shallow water (about 6 m) for temperature and fish and crab larvae in June–July 1992. These larvae were more abundant in fronts than in parcels of water preceding or following the front. Peaks in larval abundance were accompanied by a sharp rise in temperature, in itself evidence for onshore transport of surface water. It is concluded that both warm-water fronts and internal tidal bores play a key role in the exchange across the shelf of material and water properties, and that internal tidal-bore phenomena explain well the transport of both water-column and neustonic larvae in different habitats.

1. Introduction

Cross-shore circulation (i.e., perpendicular to the coastline) is a key element in the exchange of material and water properties between the coastal ocean and the nearshore (30 m and shallower). Cross-shore circulation exchanges nutrients, food, and planktonic larvae. Because cross-shore scales of some ecological phenomena are

1. Scripps Institution of Oceanography, University of California, San Diego, La Jolla, California, 92093-0208, U.S.A.

2. Present address: Biology Department, Woods Hole Oceanographic Institution, Woods Hole, Massachusetts 02543, U.S.A.

much smaller than corresponding along-shore scales (e.g. Denman and Powell, 1984; Mullin, 1986), cross-shore circulation probably has a disproportionate influence on nearshore ecosystems. An important problem in nearshore oceanography, then, is to identify the mechanisms dominating cross-shore transport processes.

Internal-tides might be important in exchange across the shelf because, as opposed to other physical forcing mechanisms, they are very energetic in the cross-shore direction. Internal tides are internal waves of tidal frequency that result from the interaction of the barotropic tide with variable topography in a stratified water column (Baines, 1986, for a review). To illustrate how internal waves could produce significant advection, consider the analogy of internal waves and surface waves. Surface waves produce insignificant advection when they occur in deep water. When surface waves enter shallow water and their amplitude becomes non-negligible with respect to water depth, the waves become nonlinear and propagate forward as surf. In shallow water, surf can produce considerable advection. In a manner similar to surface waves, internal waves produce little advection in deep water. Just as surface waves propagate forward as surf in shallow waters, internal waves also become nonlinear, break, and propagate forward as internal surf or internal bores. Surface waves usually have smaller amplitude than internal waves. While surface waves break close to the shoreline, internal waves can break relatively farther from the shore (for internal waves examples see Cairns, 1967; Emery and Gunnerson, 1973; Haury *et al.*, 1979; Shea and Broenkow, 1982).

Internal waves and bores have been observed in a number of studies in the Southern California Bight (Ewing, 1950a,b; Arthur, 1954; LaFond, 1962; Lee, 1961; Cairns, 1967; Emery and Gunnerson, 1973; Winant, 1974; Winant and Olson, 1976; Shea and Broenkow, 1982; Pineda, 1991). Internal motions are most energetic in spring and summer when the water column is well stratified. They are least energetic in fall and winter when stratification is weak (Cairns and Nelson, 1970; Winant and Bratkovich, 1981; Pineda, 1991). Internal tidal waves and bores advancing onshore can have amplitudes of up to 120 m (Summers and Emery, 1963; Emery and Gunnerson, 1973; Shea and Broenkow, 1982). It is not known where the generation site for the Southern California internal tide is. Maximum cross-correlations between sea level and temperature occur at a 3–5 hour lag in a location close to La Jolla, California (Cairns and LaFond, 1966), and 5 lag hours at the Scripps Institution of Oceanography pier (temperature close to the bottom; own unpubl. data). Advection by breaking internal waves might be important in a variety of environmental phenomena; there is only scant information, however, on the effects of internal bores in the coastal and nearshore ocean. Studies have concentrated in the Southern California Bight (but see Chapman *et al.*, 1991), where the sudden ascent of the thermocline has been related to internal bores (Arthur, 1954; Stevenson and Gorsline, 1956; Summers and Emery, 1963; Emery and Gunnerson, 1973; Winant and Olson, 1976). Cairns (1967) described internal tidal waves becoming asymmetric

when entering shallow water, and Winant (1974) observed nearshore broken internal waves propagating as surges of cold water, and he proposed that the internal bores might be strongly three-dimensional. Pineda (1991) proposed that internal tidal bores produced upwelling by advecting subsurface water to the nearshore; that several consecutive large events occurred at semidiurnal or diurnal periodicities; that effects on surface temperature lasted days; and that internal tidal bores were, on average, predictable, demonstrating a spring-neap "internal tidal cycle" not in phase with the surface spring-neap tidal cycle.

Internal-wave phenomena have been invoked to explain the onshore transport of planktonic larvae. Most benthic marine invertebrates have life cycles which include planktonic larvae. Planktonic larvae of nearshore taxa reside from minutes to months in the water column and are often dispersed and/or transported to offshore waters. To settle near the shore and complete their life cycle they must exploit physical mechanisms to return there. Hypotheses that invoke internal-wave phenomena for the onshore transport of larvae have focused on both neustonic larvae (surface-dwelling) and water-column larvae (planktonic larvae residing between bottom and sea surface). Shanks (1983), Jillett and Zeldis (1985), Kingsford and Choat (1986), Shanks and Wright (1987), and Shanks (1988) have proposed that surface slicks associated with internal waves transport neustonic larvae onshore. The hypothesis is that surface slicks, created by surface convergent currents generated by internal waves (Ewing, 1950a,b), concentrate neustonic larvae able to swim upward faster than the downward convergent currents. As internal waves advance onshore, the accompanying slicks would also transport their trapped material shoreward. The internal-tidal-bore hypothesis (Pineda, 1991) states that water-column larvae are transported shoreward by large internal tidal bores. According to the hypothesis, the transported larvae should be found in the thermocline or close to the bottom where the thermocline intersects the sea floor. Shoreward-breaking internal waves at the thermocline would thus produce nearshore upwelling by transporting subsurface masses of water together with larvae occurring there.

If internal tidal bores cause upwelling, then the advection of dense subsurface water to the shoaling nearshore should create a horizontal imbalance in hydrostatic pressure between dense inshore surface water and lighter offshore surface water. This might produce an onshore surface flow of lighter water and a seaward bottom flow of heavier water. Such a baroclinic flow could transport neustonic larvae onshore. (Here, baroclinic is used for currents that reverse with depth.) This could also help to explain Arthur's (1954) brief description of a puzzling shoreward movement of a warm-water front observed from the Scripps Pier (see Discussion). These phenomena are consistent with the hypotheses offered in this paper: namely, that subsurface dense water advected onshore by large-event internal tidal bores produces a subsequent baroclinic flow, in which the dense nearshore water slides downslope seaward as a gravity current, setting up the onshore advection of the

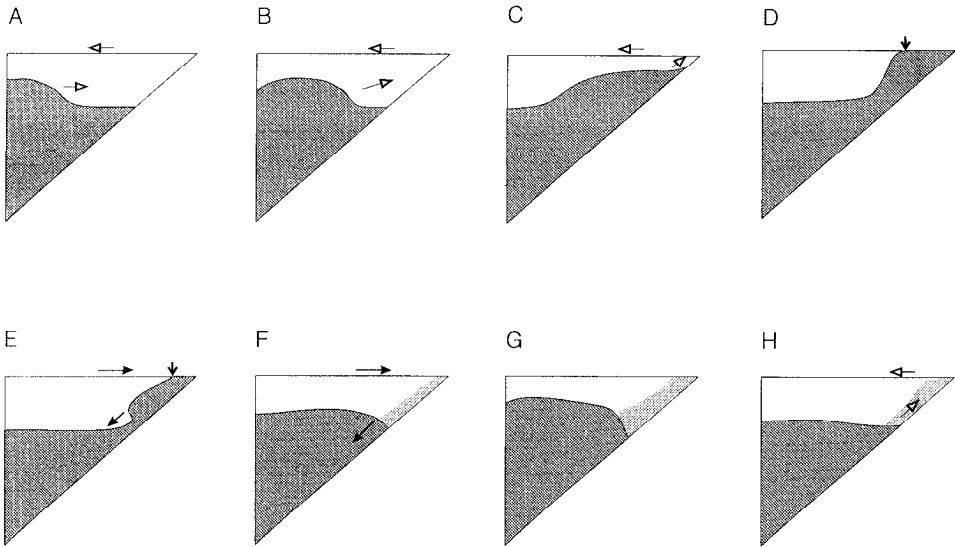


Figure 1. Graphical model of the onshore advection of a dense water body (panels A–C), followed by its subsequent down slope progression and the corresponding onshore advection of a warm-water body (panels E–H). Dotted regions represent denser water. Triangular sections represent cross-shore profiles. The vertical arrow represents position of warm-water front in panels D and E, and the other arrows represent currents. Horizontal scale greatly reduced relative to vertical scale. Panels A–C represent “phase one,” while panels E–H represent “phase two.” (See under “Del Mar: Results” for an explanation.)

surface warm water. As cold water upwells into warmer water, water-temperature fronts form (Fig. 1). This is used as background for the ecological hypothesis, which states that shoreward flow transports onshore neustonic larvae in concentrating warm-water fronts.

This paper analyzes events in which temperature fluctuations are accompanied by energetic cross-shore currents that could influence onshore transport of larvae. To illustrate how temperature is related to currents in these events, data from a 1978 physical oceanographic study are used (the “Del Mar” data). Analysis of these observations demonstrates a correlation of temperature fluctuations with advection. Another data set of temperature alone (the “Scripps Pier” data), is used to identify similar events, to infer cross-shore advection, and to characterize a basically undescribed phenomenon: the onshore migration of warm-water fronts. The phenomenological description of these advective events is then used as the necessary background to test the ecological hypothesis, the onshore transport of neustonic larvae in warm-water fronts, using data from an ecological experiment (the “Transport of Neustonic Larvae” temperature and larva data). This work focus on analysis of observations. A quantitative description is beyond the scope of the present contribution.

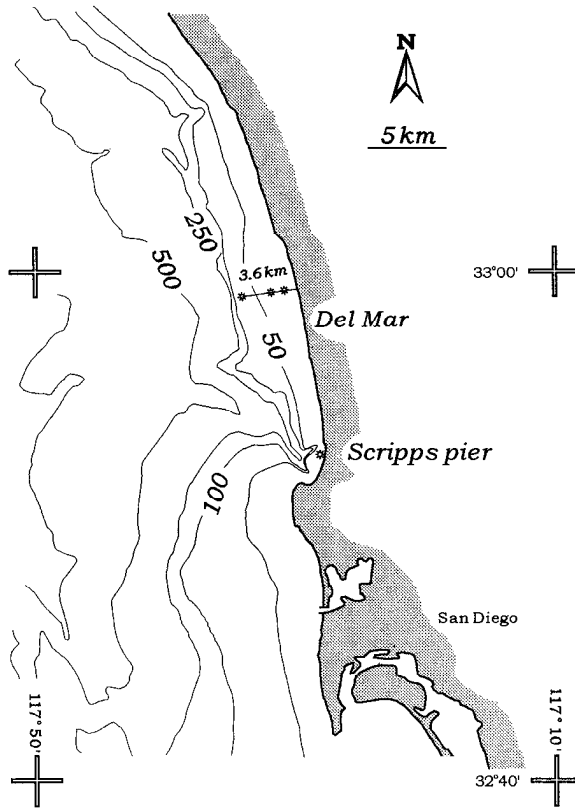


Figure 2. Study sites. Isobaths in meters.

2. Methods, results and interpretation

This section describes (1) current and temperature data from Del Mar, Southern California (Fig. 2); (2) temperature fluctuations at the Scripps Pier, about 11 km south of Del Mar (Fig. 2), and (3) ecological experiments at the Scripps Pier. The Del Mar data set is used because it includes current and temperature observations at three stations over the shelf. Temperature observations at the Scripps Pier are used because (1) high-frequency temperature data are available since mid 1987; (2) surface water temperature measurements are available; (3) visual observations were made at this location; (4) a 60 year historical daily-temperature time-series is available, and (5) ecological studies were conducted at this location. The Del Mar and Scripps temperature and current data are interpreted before describing the hypotheses, rationale, and methodology of the ecological studies. This sequence was chosen because the interpretation of the physical phenomenon, energetic cross-shore advection, is necessary to understand the design and rationale of the ecological experiments.

a. Del Mar: methods. The Del Mar data set is described by Lentz and Winant (1979). The site was selected because of its relatively simple topography (Fig. 2). The instrument arrays were moored on a smooth sloping shelf; seaward of the 60 m isobath, the slope steepens abruptly. The deployment worked intermittently during 1978–1979. Observations reported here were selected from the interval spanning from 27 July to 10 September 1978. Current meters and temperature sensors were deployed at three stations perpendicular to the coastline in water depths of 15, 30, and 60 m. The 60 m station was about 3.6 km from the coastline. The 60 m station had instruments at 4, 18, 32, 43 and 55 m water depths; the 30 m-devices were at 3, 12, 19 and 27 m, and those at the 15 m station were at 3, 8 and 12 m. Data were sampled every 2 min. but hourly averages were reported. Along-shore and cross-shore currents were measured with Vector Measuring Current Meters. Along-shore and cross-shore direction are defined as parallel and perpendicular to the isobaths (parallel to 335°T and 65°T). Temperature observations had $\pm 0.05^\circ\text{C}$ accuracy. In this region, alongshore barotropic currents likely produced by the semidiurnal surface tide have amplitudes on the order of $10\text{--}20\text{ cm s}^{-1}$ (Winant and Olson, 1976; Winant and Bratkovich, 1981).

b. Del Mar: results. Four events are described. Events are defined as a cooling of the water column at the shallowest station accompanied by an onshore current close to the bottom and a seaward surface flow (“phase one”). This is followed (“phase two”) by warming of the water column and current relaxation and reversal at the shallowest station (15 m). This paper focuses on “phase two,” which exhibits relatively more energetic flows, seaward close to the bottom and onshore at surface.

The first 3–5 panels of Figures 3–6 (panels 0 h to 2 h–4 h) show phase one, with onshore currents close to the bottom and seaward currents close to the surface at all three stations. For each event, maximum onshore bottom current speeds range was $6.2\text{--}8.3\text{ cm s}^{-1}$, while maximum seaward surface current range was $6.1\text{--}15.1\text{ cm s}^{-1}$. In panels 2–4h, the currents relax and reverse at the 15 m station. Phase two follows, featuring seaward bottom currents ($8.9\text{--}20.1\text{ cm s}^{-1}$; maxima) and onshore surface flow ($12.1\text{--}17.9\text{ cm s}^{-1}$; maxima). In phase one, maximum onshore and seaward speeds during each event occur at different instruments within the stations. The same is true for onshore surface flow at phase two. However, seaward bottom currents at phase two consistently occurred at the shallowest station at the instrument closest to the bottom.

For all events, temperature at the shallowest or deepest sensor of the 15 m station in phase one dropped ca. $1\text{--}4^\circ\text{C}$, while it rose ca. $1.5\text{--}5^\circ\text{C}$ during phase two. Isotherms rose during phase one and became horizontal. A noteworthy characteristic of the events during phase two is that isotherms bend downward sharply between the 15 m and 30 m stations (panels 5–6h, Fig. 3; panel 6h, Figs. 4 and 5; panels 5–6h,

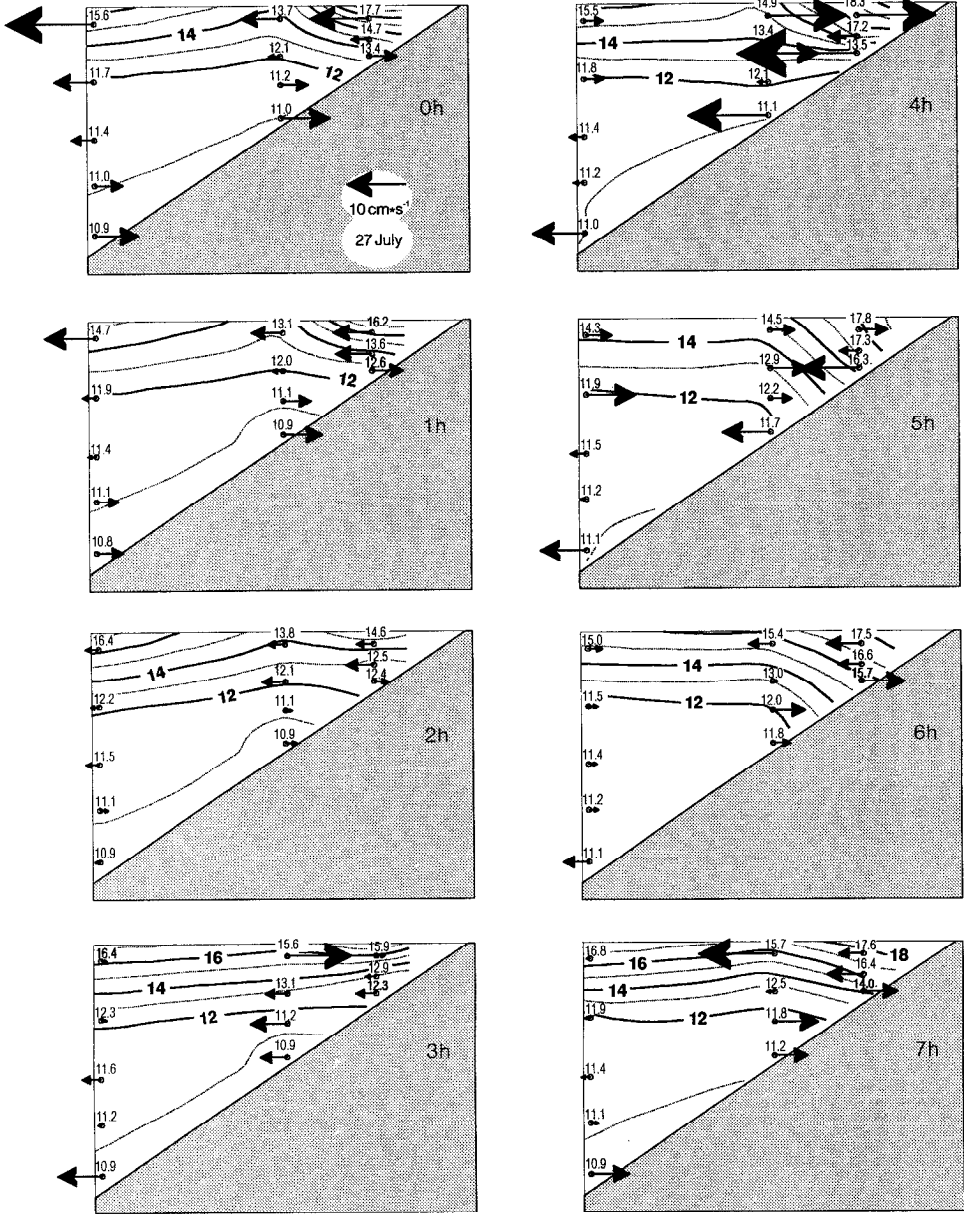


Figure 3. Isotherms and current speeds at one hour intervals at stations in 15, 30 and 60 m water depth off Del Mar, California on 27 July 1978. Small circles show scaled instrument position and small nearby numbers are actual temperature readings. Bold numbers are values for interpolated isotherms. Arrows pointing right represent onshore (65° relative to true north) currents. Arrow size is proportional to current speed. Instrument depths at the 60 m, 30 m and 15 m stations were 4, 18, 32, 43 and 55 m; 3, 12, 19 and 27 m; and 3, 8 and 12 m, respectively.

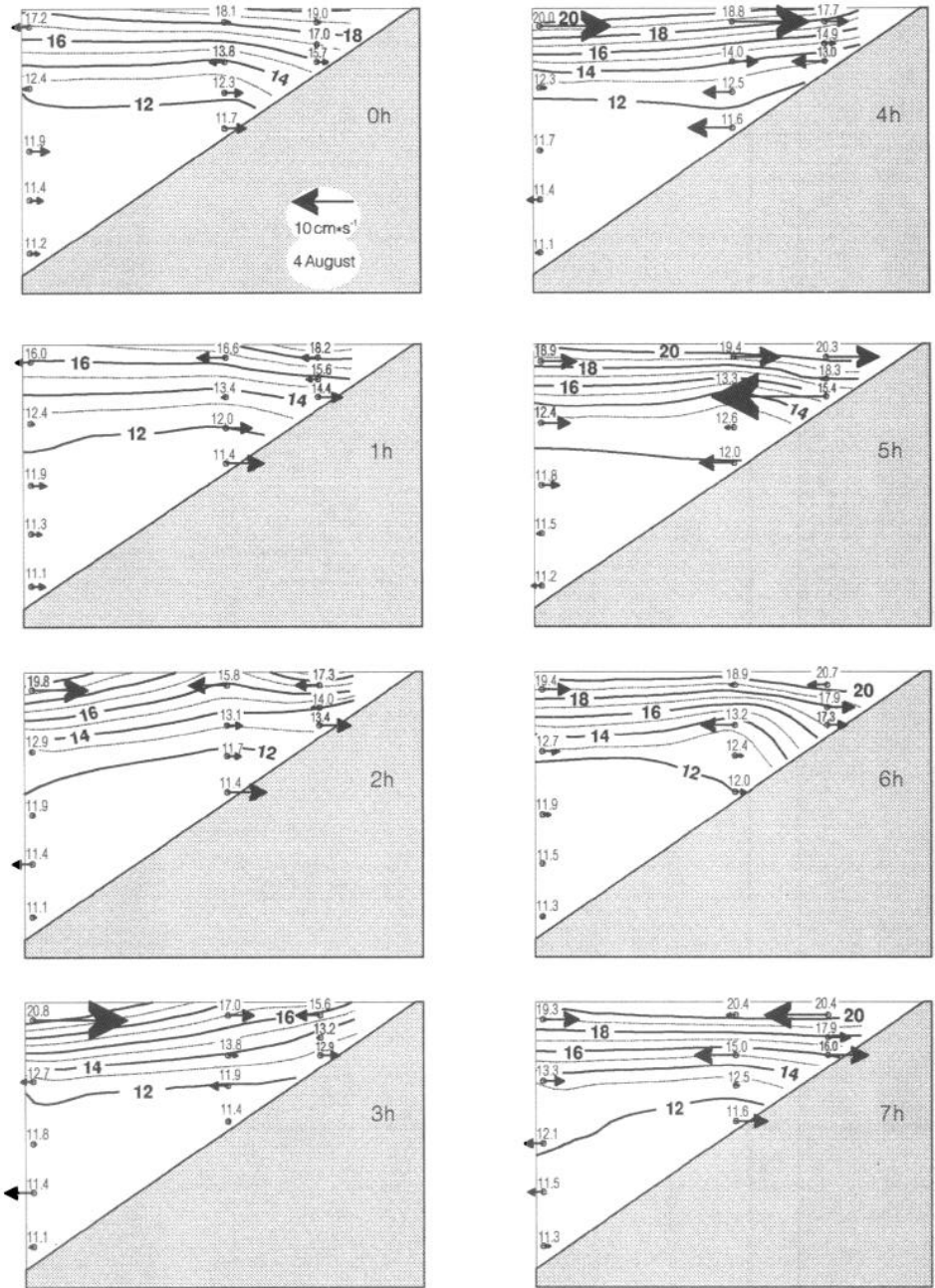
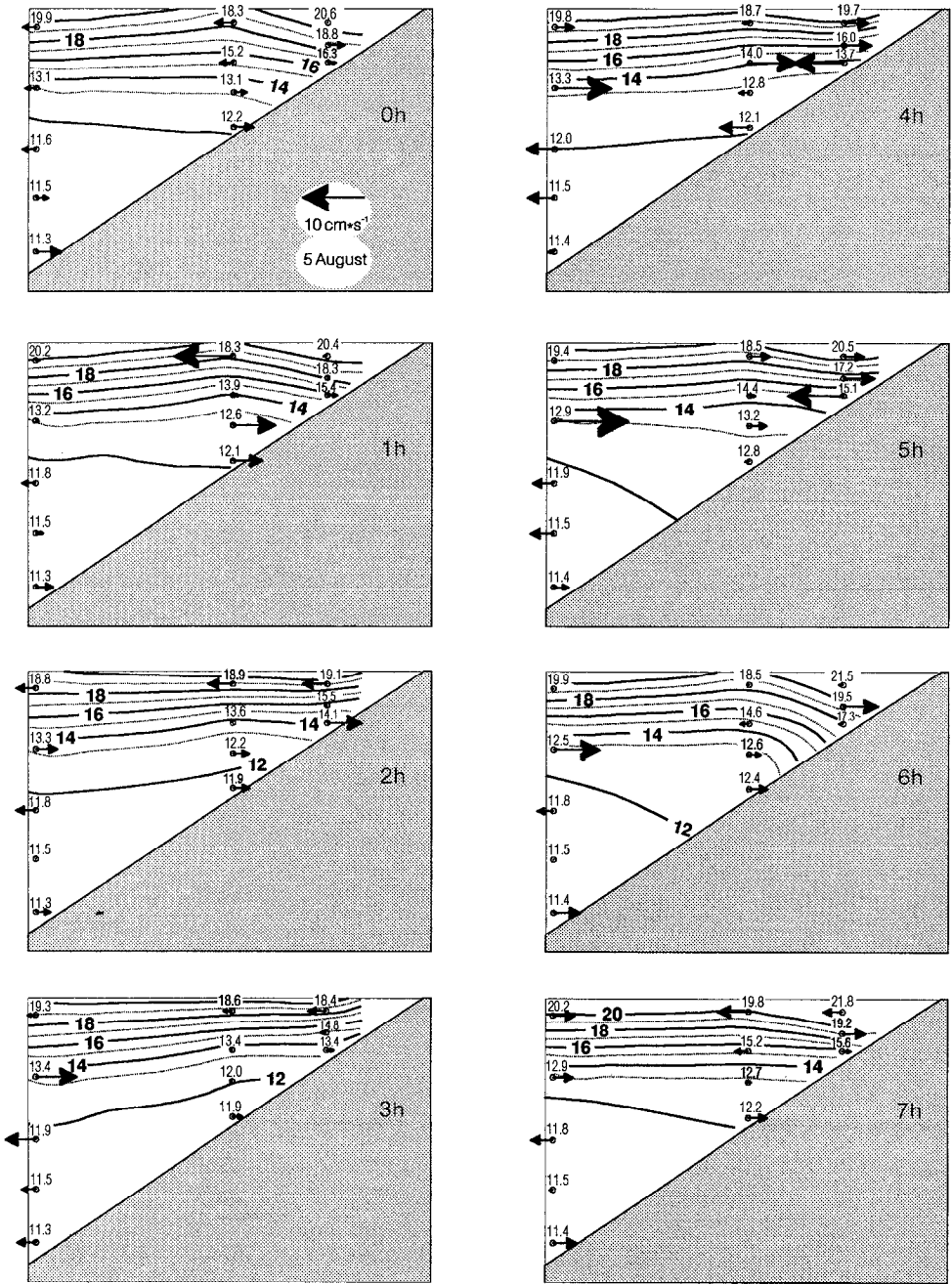


Figure 4. Isotherms and current speed vectors at stations 15, 30 and 60 m off Del Mar, California on 4 August 1978. Symbols as in Figure 3.



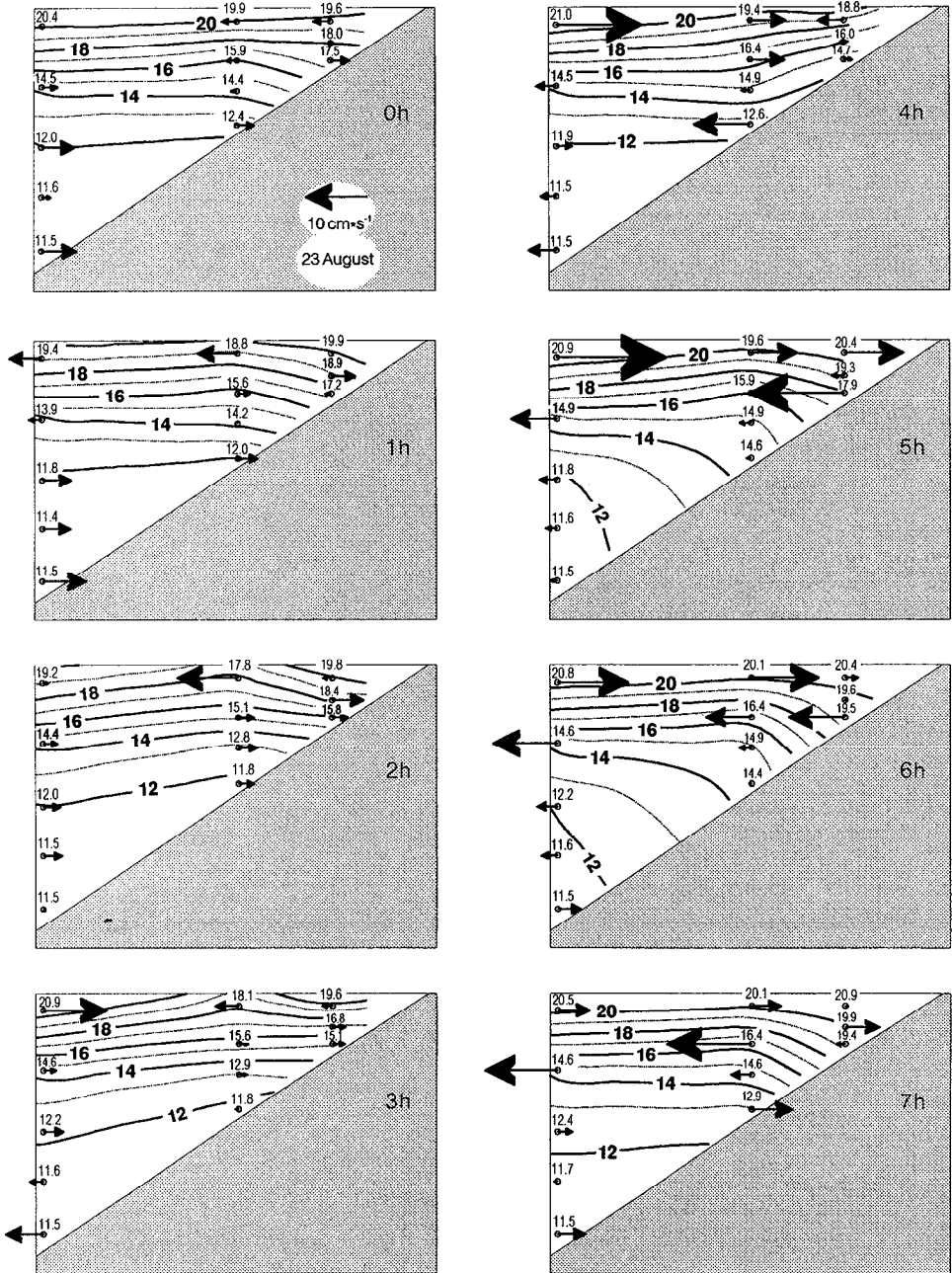


Figure 6. Isotherms and current speed vectors at stations 15, 30 and 60 m off Del Mar, California on 23 August 1978. Symbols as in Figure 3.

Table 1. Observed average time scales for events at Del Mar (Figs. 3–6). Currents at 3 and 12 m had similar scales. Numbers in parentheses are number of periods (T) used to calculate the average scales. In some cases periods from minima to minima and from maxima to maxima were both used to calculate periods.

Event	Currents	Temperature (12 m depth)	Temperature (3 m depth)
1	7 h (3)	6 h 15 min (4)	14 h (1)
2–3	5 h 55 min (11)	5 h 50 min (10)	12 h (4)
4	5 h 24 min (5)	5 h 30 min (6)	12 h 15 min (4)

Fig. 6). In one case (Fig. 6) some isotherms bend between the 30 and 60 m station. Temperature varied most at the 15 m station.

The time scales of the current and temperature events were calculated from the series by averaging the time interval between minima and between maxima at the 15 m station. To compute the measurements over entire periods (T = period between minima or between maxima), values of the series not plotted in Figures 3–6 were also used. Scales for currents were similar at the deepest and shallowest instruments (12 and 3 m water depths) and were close to double semidiurnal (Table 1) but those for bottom and surface temperature were different. Temperature close to the surface had frequency close to semidiurnal, while bottom temperature scales had frequency close to double semidiurnal (Table 1).

Figure 7 shows mean currents over 24 hours for events in Figures 3–6, and mean currents over 24 hours averaged over all events. (See Fig. 7 for details.) In general, mean surface currents are directed onshore at the 15, 30 and 60 m stations. A mean onshore current also occurs consistently at the bottom in stations 30 and 60 m, whereas at the 15 m station the mean bottom currents are consistently directed offshore. Two exceptions to these flow patterns occur at 60 m and at 30 m for surface currents (Fig. 7, panels 1 and 4), and at the 60 m station for the bottom flow (Fig. 7, panel 1).

c. Scripps Pier: methods. Temperature observations at the Scripps Pier (Fig. 2) were made in summer and fall 1990; the record is part of the Scripps Pier automatic weather station (SPAWS). Two sensors located about 300 m from the coastline in 6 m of water (on average) record temperature at 5 min. intervals. One sensor is located about 1.5 m above the bottom (bottom depth changes due to erosion and accretion of sand), the second sensor is about 3 m above the bottom sensor (about 0.5 m below the lowest water level). These sensors will be referred to as bottom and subsurface. Surface water temperature measurements on 28 June were recorded by a floating device separated longshore by about 15 m from the water-column sensors. Surface water temperature measurements at various fixed distances from the shore were obtained by sampling surface water with a bucket from the Scripps Pier. All times given are GMT.

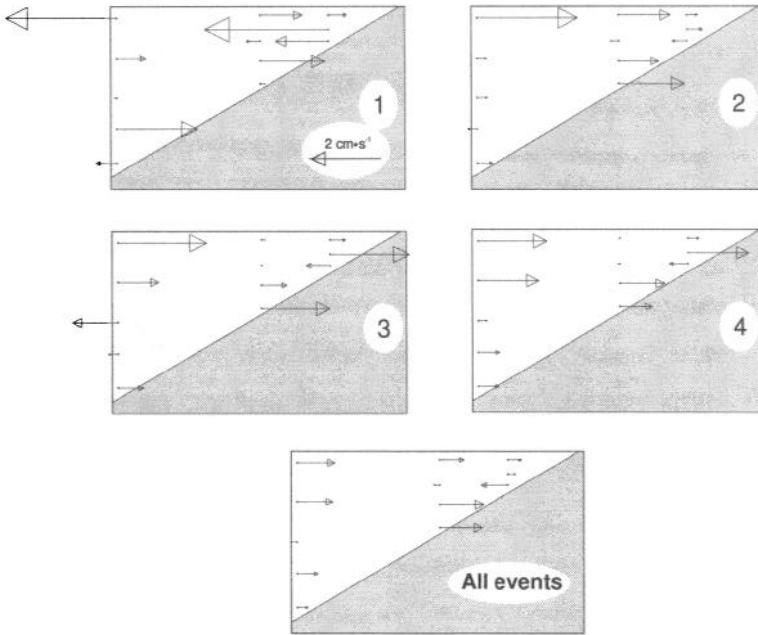


Figure 7. Mean currents over 24 h for events in Figures 3–6 and mean currents over 24 h averaged over all events. Panels 1, 2, 3, and 4 correspond to events in Figures 3, 4, 5, and 6. The 24 hours averages for panels 2, 3 and 4 included data from 8 hour “before” the events, the observations corresponding to the events, and data 8 h “after” the events. For panel 1, the 24-h average was calculated from data included in Figure 3 and from 16 h of data after the event. This was done because for this event there are no “before” observations. Symbols as in Figure 3.

d. Scripps Pier: results. Two events, defined as a sudden rise (within 0.5–1.5 h) in subsurface and bottom water temperature, are described. These were chosen because surface temperature measurements were also available. Both the 21:00–June 28 and the 17:30–November 2, 1990 events were preceded by a 4–6°C drop from background bottom and subsurface water temperature (Figs. 8, 9). The increase in temperature that followed was about 5°C on June 28 and 3°C on November 2. Bottom and subsurface temperature behaved similarly throughout the events. The shape of the temperature trace is asymmetrical, with the falling temperature trace less steep than the rising portion (Figs. 8A, 9A). On both June 27–30 and November 2–4 several events occurred; the group of events appear to have semidiurnal periodicity in June and diurnal in November. Nearshore water column stratification was strong on June 28 and weak on November 2.

e. Scripps Pier: surface expression. On occasion a visible surface front accompanies the events. In both cases described here, measurements revealed shoreward moving fronts dividing bodies of water of different temperature, with that closer to shore

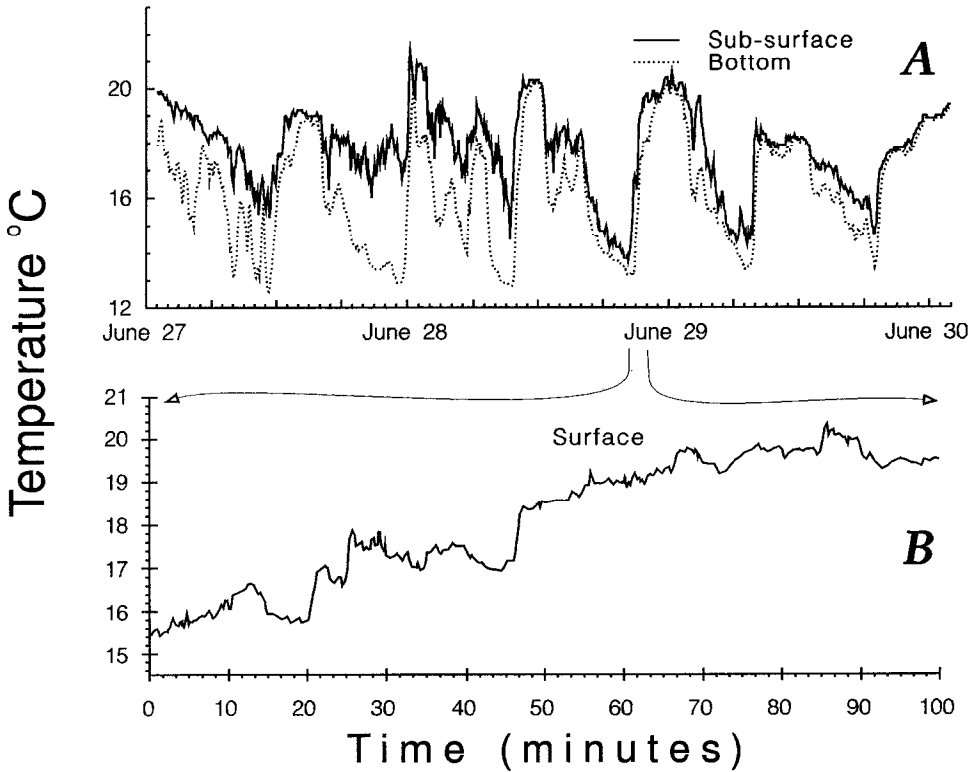


Figure 8. Temperature observations at the end of Scripps Pier in 28 June 1990. Panel A. Temperature sensors were located about 300 m from the shoreline in water of about 6 m depth (on average) and sampled every five minutes. The bottom (broken line) and subsurface (solid line) sensors are about 1.5 m and 4.5 m above the bottom. Panel B. Surface water temperature measurements; temperature was recorded at high frequency and then the record was sub sampled at ca. 1–2 readings per minute. Time 0 is about 20:30 June 28. Time in GMT.

colder than the one offshore. Both fronts disappeared somewhere in the surf-zone. For both cases, at least one foam band 3–10 m wide aligned parallel to the coastline separated water bodies of different color; the bands contained accumulations of foam, kelp, surfgrass, plastic and other debris at the surface and in the front at least 1–2 m deep. The foam band on June 28 was associated with an unquantified sharp temperature gradient.

When the 28 June front was first seen, it was about 500–1500 m from the shoreline and appeared to have a broad longshore extent. Figure 8B shows the surface water temperature record when the front reached the Scripps Pier. The surface temperature rose from 15.7 to 19.9°C in 1 h. The temperature trace is characterized by three sudden increases, which account for most of the temperature rise during the interval considered. The sharpest rise is of about 1.5°C in less than 2 min. One reversal in

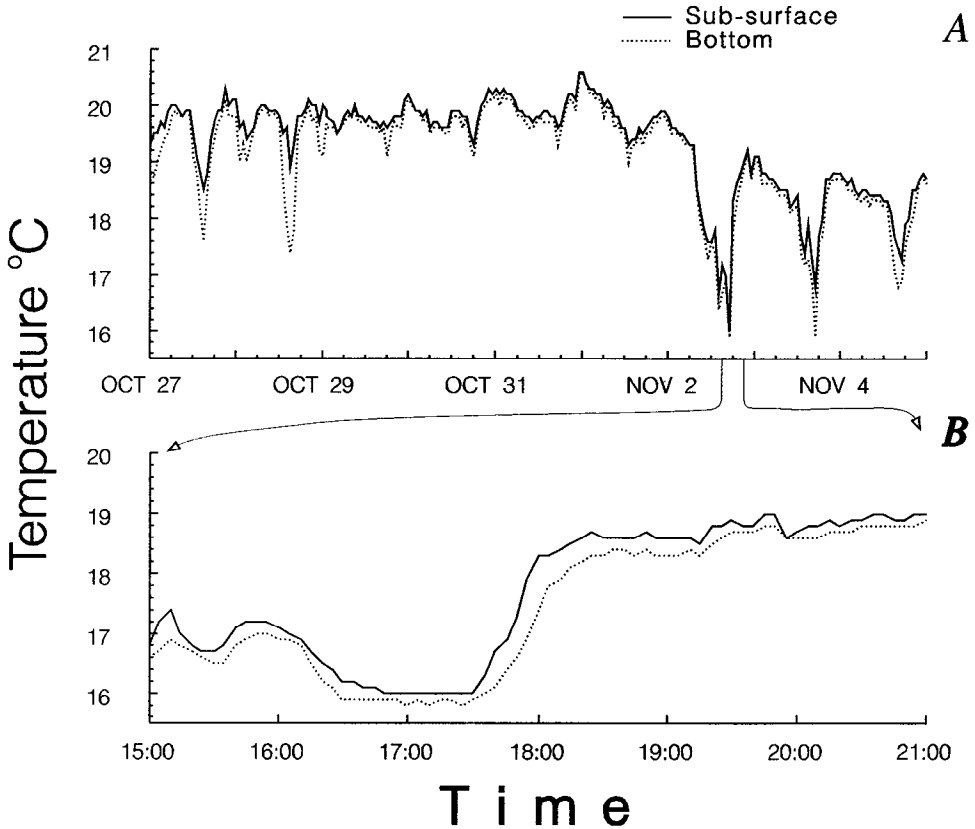


Figure 9. Temperature observations in Fall, 1990. Temperature was sampled each hour for A, each 5 minutes for panel B. Panel B is an expansion of Panel A for 2 November. Location and symbols as in Figure 8 panel A.

temperature is also apparent. The 2 November front was about 300 m from the shoreline when first seen. A transect from the Scripps Pier across the front showed a single temperature difference of 1.1°C over a horizontal distance of about 9 m (Fig. 10A); a second transect undertaken shortly after the first one showed that the front had moved shoreward (Fig. 10B). More observations on fronts will be discussed under the section "Transport of Neustonic Larvae: Results."

f. Del Mar and Scripps Pier: interpretation. The Del Mar events (Figs. 3–6) are interpreted as shoreward advection of subsurface water replacing nearshore water (phase one); this produces upwelling in the nearshore. This is followed by warming of the whole, shallow water column at the 15 m station accompanied by energetic seaward bottom currents and onshore surface flow (phase two). The sudden increases in temperature at Scripps Pier (Figs. 8; 9) are interpreted as the replacement of nearshore dense water by lighter water over short time spans (about 0.5–1.5 h).

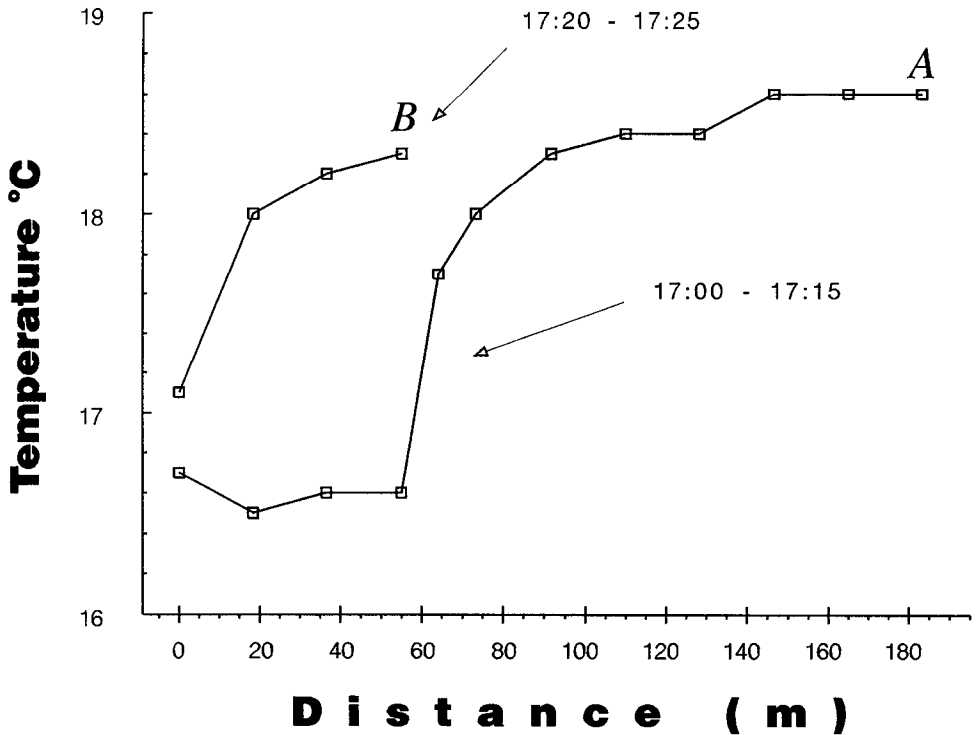


Figure 10. Transects of surface water temperature measured from Scripps Pier on 2 November starting at 17:00 (A) and 17:20 (B). Distance 0 is closest to the shoreline and corresponds to Scripps Pier pile number 16, then located near the seaward edge of the surf zone. Time in GMT.

The events occurred after a drop over 4–8 h in subsurface and bottom water temperature from background levels. These drops, and the similarity of the Del Mar and Scripps events, will be taken up later, in the discussion.

The fact that the Scripps Pier bottom and subsurface temperatures are similar and vary together implies that the oscillation in temperature is not due to vertical displacement in the water column, but instead due to cold water advecting to the shoreline and then being replaced by a warm-water body. Between June 28 and June 30 the cold-water body was replaced four times, while it was replaced three times from November 2 to 4. The surface water temperature measurements and visual observations support this interpretation.

A schematic model of the advection of the warm-water body at Scripps Pier on June 28 is presented in Figure 11. The diagram in Figure 11 is not directly comparable to the Del Mar Figures 3–6 because Figure 11 represents a shallower nearshore water column and because cross-shore patterns (such as isotherm flattening and downtilting in Figs. 3–6) cannot be derived from data from only one station.

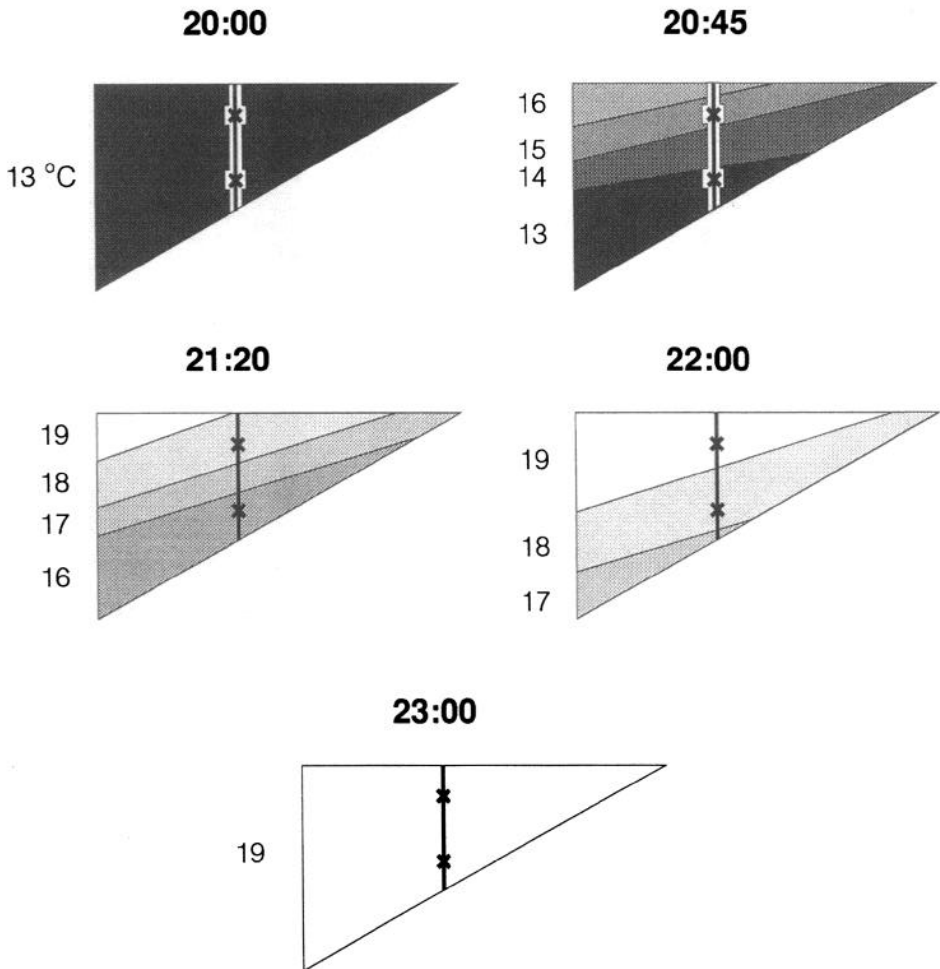


Figure 11. Schematic model of the replacement of a cold water body by a warm water body on 28 June 1990. X's represent temperature sensors. Triangular sections represent cross-shore profiles.

The model assumes that the bottom and sub-surface sensor temperatures are actually equal to the water temperatures at the sea-air interface and at the bottom. Another assumption is that the phenomenon is two-dimensional (see below). Figure 11 shows that temperature fluctuations on June 28 are consistent with advection. Sharp temperature differences at the surface suggest a horizontally tilted thermocline in a water column, as shown in Figure 11. This subsurface temperature gradient is consistent with the idea that the advected waters were thermocline waters.

g. A gravity current. Consider a model basin which is shallow, nearshore, and with moderate sloping topography and two water bodies of different densities, the denser water being trapped between the shoreline and the offshore lighter water mass (an example with these initial conditions is discussed below). Rotation effects are not considered here. A horizontal density gradient would produce a corresponding horizontal hydrostatic pressure gradient. This might produce a baroclinic flow in which the densest water would slide downslope and retreat offshore and, for continuity, the lighter water would move shoreward. If density differences are determined by temperature, then the shoreward moving gravity current could produce a warm-water, shoreward moving front.

This problem, the mutual intrusion or lock exchange flow, has been solved by equating decrease in potential energy with increase in kinetic energy (O'Brien and Chernov, 1934). The downslope speed U of the seaward bottom current can be roughly calculated under the assumption that the events in Figures 3–6 were gravity currents propagating down slope with corresponding onshore surface flow. The speed of advance of the current U can be calculated using the formula of Simpson (1987):

$$U = 0.5 \sqrt{\frac{\Delta\rho}{\rho} gH}$$

where ρ is the density of the light body, $\Delta\rho$ is the density difference between the two bodies, H is the mean height of the dense current and $g = 9.81 \text{ m s}^{-2}$. The nearshore shelf slope is smaller than 1° and thus it is convenient to assume a gravity current propagating along a horizontal surface.

Density variability in the vicinity of La Jolla is mainly determined by temperature variability (e.g. Winant and Bratkovich, 1981). For the Del Mar events (Figs. 3–6), assuming a salinity value of 33.6% (Cairns, 1967) temperature differences averaged over the water-column between the end of phase one and the start of phase two at the 15 m station yield $\Delta\rho$ between 4.5×10^{-4} and $8 \times 10^{-4} \text{ g cm}^{-3}$. Assuming that these represent $\Delta\rho$ of a gravity current and an $H = 750 \text{ cm}$ (the mean depth from the 15 m station to the surfzone), calculated values of U range from 9.0 to 12.0 cm s^{-1} (Table 2).

Averaged values for the observed seaward bottom current (phase two) offer a rough check for the model values. Observed values, calculated only from the deepest (12 m water depth) instrument, range from 8.5 to 11.9 cm s^{-1} . The rank order of the current speeds corresponds in the calculated and the observed values (Table 2). Similar calculations for the Scripps data assumed a similar H and calculated $\Delta\rho$'s from the observed differences between the lowest temperature in the cold-water event and the highest temperature of the incoming warm-water body. The calculated U was 14.4 cm s^{-1} for June 28 and $U = 9.5 \text{ cm s}^{-1}$ for November 2.

Table 2. Calculated and observed current speed U for the Del Mar events at the 15 m station during phase two (see "Del Mar: Results," for a description). Events 1–4 correspond to Figures 3–6. Averaged offshore U includes all currents at the 12 m-depth instrument only. Averages were obtained from data in Figure 3–6.

Event	Calculated U (cm s ⁻¹)	Observed averaged offshore U (cm s ⁻¹)
1	11.0	11.2
2	12.0	11.9
3	9.0	8.5
4	10.8	8.6

h. Transport of neustonic larvae: hypothesis. The hypothesis that shoreward flow transports neustonic larvae in concentrating warm-water fronts predicts that larvae will be most abundant in convergent zones where strong horizontal temperature gradients occur. Warm-water fronts, like those described here, can be identified by high concentrations of floating debris (personal observation). Debris accumulation could be evidence for convergent currents, because it should be produced by some sort of concentrating mechanism, as the frontal convergent currents described for other frontal systems (Le Fèvre, 1986 for a review). If the inferred convergent currents concentrate debris, then they could also concentrate neustonic larvae. The prediction that concentration should take place at strong horizontal temperature gradients contrasts with other concentrating phenomena such as Langmuir circulation or internal wave slicks. Lastly, the diurnal or semidiurnal frequency of the temperature oscillations is a distinctive character of these events.

i. Transport of neustonic larvae: methods. Fish and crab neustonic larvae, together with surface-water temperature, were sampled at the end of Scripps Pier in Summer 1992. A 300 μ m-mesh neuston net (0.343 m width \times 0.310 m height mouth aperture) half immersed in the water was used to complete two transects at about 6 m water depth. The two transects were either parallel or perpendicular to the shoreline (see below). Total length was 57.3 or 64.1 m, and volume filtered was 3.1 or 3.4 m³. Volume filtered was calculated as $0.5 \times \text{net mouth area} \times \text{transect length}$. Temperature measurements during plankton sampling were done with a bucket thermometer from the end of Scripps Pier. Only 1.0 m³ was filtered in the July 9 front due to net clogging.

The routine procedure started when a 3–6°C drop in bottom water temperature was detected at the SPAWS. This was followed by measurement of surface water temperature with a bucket thermometer; if a drop in surface water temperature had also occurred, then the sampling procedure continued. The sampling protocol included measuring surface water temperature with a bucket thermometer throughout the event and sampling neustonic plankton (the transects described above) before the front (in colder water), in the front and after the front (in warmer water).

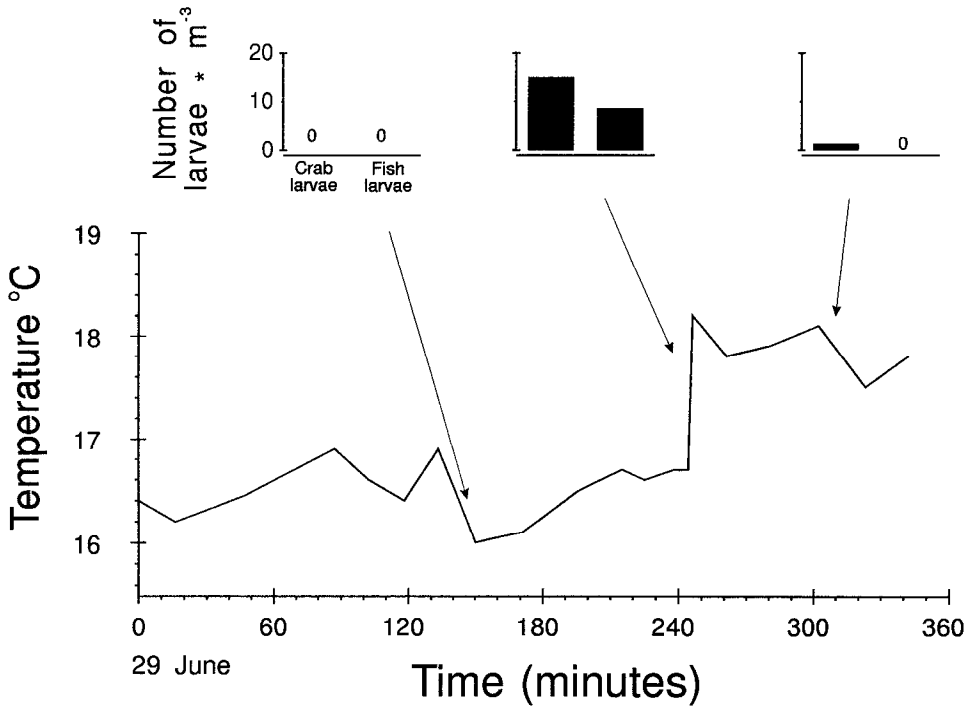


Figure 12. Neustonic larva abundance and surface water temperature at the end of the Scripps Pier on 29 June 1992. Arrows denote approximate time of plankton sampling.

After detecting the front, higher-frequency temperature sampling was briefly performed and then plankton sampling would ensue. For events with two or more fronts, times “after” the first oncoming front are identical to times “before” the second front. Complete bottom and subsurface water temperature records from the SPAWS are unavailable for the sampling months.

j. Transport of neustonic larvae: results. Fronts were easily identified as linear surface features containing floating debris with strong horizontal surface-temperature gradients. Fronts included high concentrations of debris from the surface, to at least 1–2 m deep. Some fronts arrived parallel to the coastline, but others bent and were perpendicular to the shoreline when crossing Scripps Pier. Some perpendicular fronts showed no bending near the Scripps Pier. Perpendicular fronts were sometimes moving northward, sometimes southward. Some were associated with unusually strong along-shore currents. Most fronts disappeared at the surf zone, where large concentrations of debris (mostly kelp) could be observed. After some events, large amounts of kelp were left stranded on the beach.

Figures 12–15 show the abundance of fish and crab neustonic larvae and surface water temperature in four events during June and July 1992. Figure 16 also shows

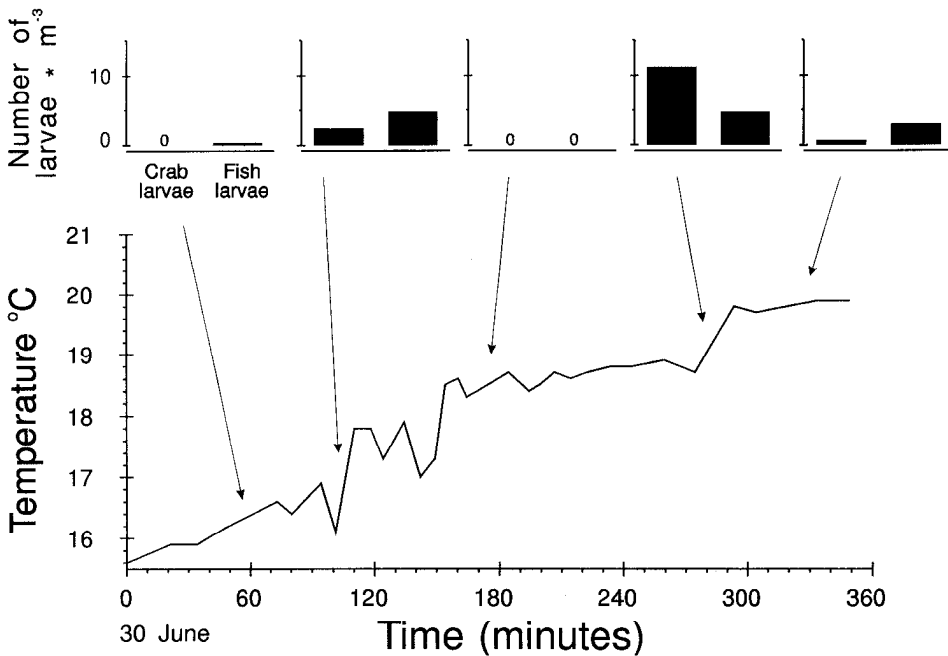


Figure 13. Neustonic larva abundance and surface water temperature in 30 June 1992. Locations and symbols as in Figure 12.

surface-water temperature observations over two sequential transects perpendicular to the coastline on July 8. The range of larval abundance was $0\text{--}15.1\text{ m}^{-3}$ for crabs and $0.7\text{--}8.5\text{ m}^{-3}$ for fish. For larvae not in fronts, the range was $0\text{--}1.3\text{ m}^{-3}$ for crabs and $0\text{--}3.3\text{ m}^{-3}$ for fish. For any event, larvae were more abundant in the fronts than after or before them. In two events (Figs. 12, 13) where larvae were sampled outside the fronts, larvae tended to be found after the fronts had passed. Maximum surface temperature difference per event ranged from about 2 to 8°C . Most events included one single front but the June 30 event (Fig. 13) had three fronts (each one of the fronts had a corresponding foam band). Figure 16 shows two temperature transects at Scripps Pier. The second transect shows relatively higher water temperature, and the warmer water is closer to the surf zone in the second transect.

3. Discussion

This section considers: (1) the nearshore cooling preceding the warm water fronts and its frequency; (2) the similarity of the Scripps and Del Mar events; (3) assumptions of the schematic model of the events; (4) some typical characteristics of the temperature fluctuations and cross-shore currents; (5) the scales of internal tidal bores; (6) the onshore transport of neustonic larvae and (7) some general implications.

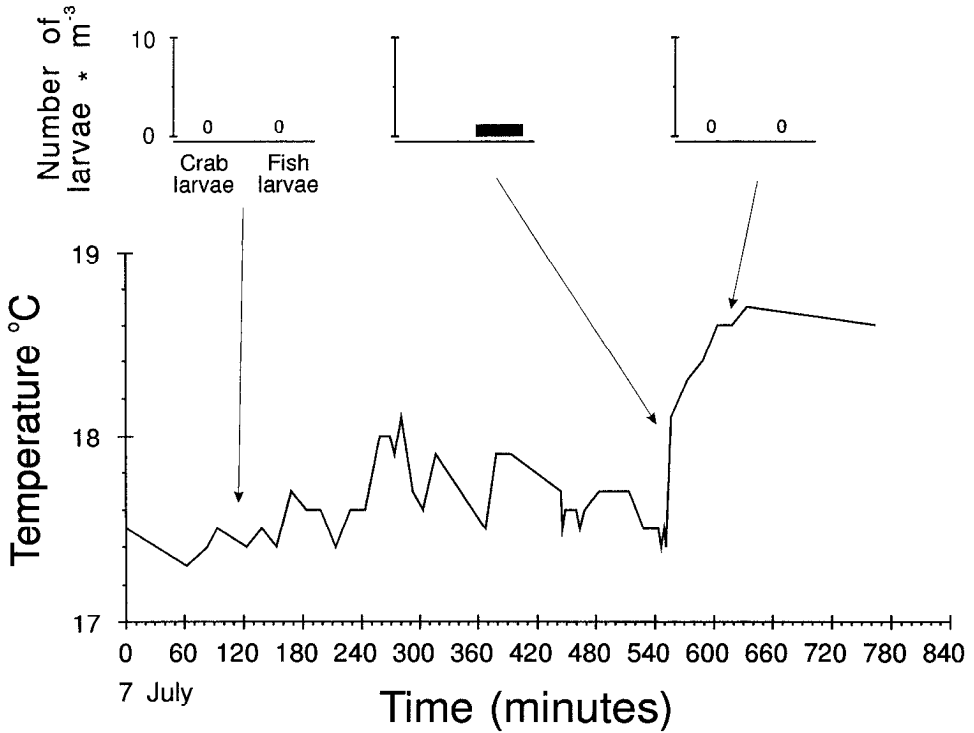


Figure 14. Neustonic larva abundance and surface water temperature in 7 July 1992. Locations and symbols as in Figure 12.

The rises in water temperature accompanying shoreward propagating warm fronts can be explained as an adjustment set up by the down-slope progression of the inshore denser water body and can be described as a return to background conditions. Therefore, the first-order phenomenon to explain is the anomalous nearshore presence of a cold water body. Large internal tidal bores can explain this phenomenon (Pineda, 1991). Figures 3–9 show temperature records that are interpreted as large-event internal tidal bores followed by warm-water fronts. It is proposed that seaward gravity currents and shoreward warm-water fronts, as described above, are epiphenomena of internal tidal bores. The SPAWS was installed in late August 1989, and many warm-water events such as those described above have been recorded. There are insufficient data to assess the frequency of these groups of events, but frequency could be inferred from the Scripps Pier historical surface water temperature record, measured every day at the seaward end of Scripps Pier since about 1920. In this time series, drops in temperature are well explained by large-event internal tidal bores; the drops are, on average, predictable, occurring mostly in spring and summer and have lunar periodicity (Pineda, 1991). Warm-water events follow

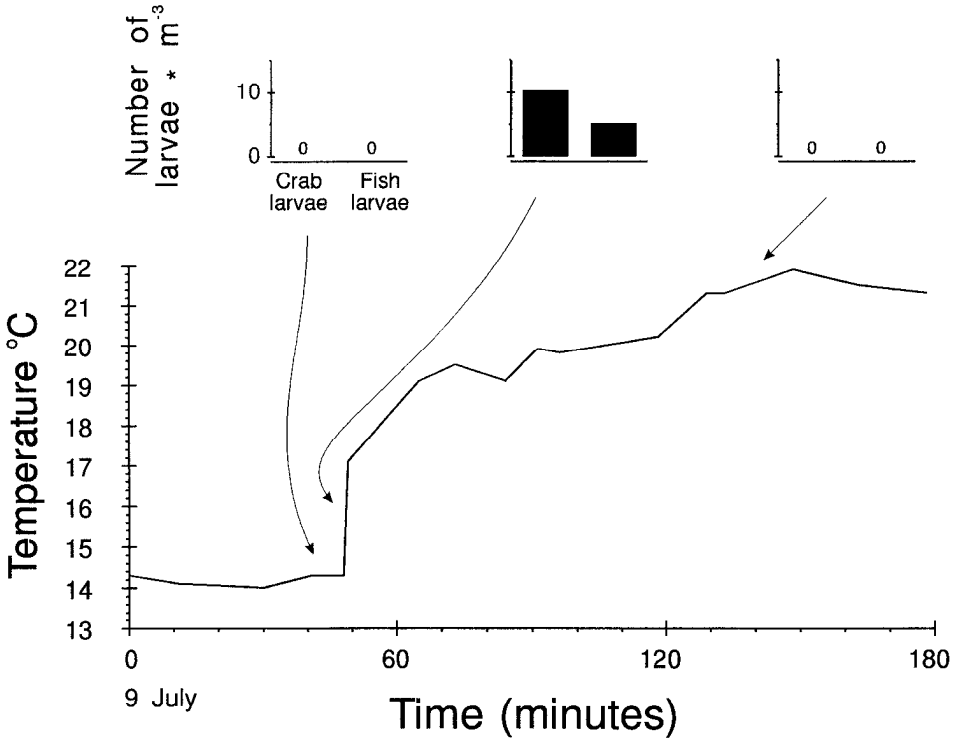


Figure 15. Neustonic larva abundance and surface water temperature in 9 July 1992. Locations and symbols as in Figure 12.

large-event internal tidal bores, and thus could be expected to have a similar periodicity.

A cooling event similar to those discussed here is described by Winant and Olson (1976), who present a time series of isotherm depth and cross-shore current speed and direction for a 17 m water-depth site off Mission Beach, about 9 km south of the Scripps Pier. Flow speeds up to about 18 cm s^{-1} were found for onshore bottom currents. For phase two, when bottom water flows offshore, maximum current speeds were about 12 cm s^{-1} for onshore moving subsurface water and ca. 34 cm s^{-1} for bottom seaward currents. (The fact the maximum speeds reported by Winant and Olson are higher than those found at Del Mar is partially due to the use of 60 min. averages at Del Mar compared with 4 min. readings at Mission Beach.) Scripps Pier is in front of a bifurcating submarine canyon (Fig. 2) that might intensify internal waves. It is well known that internal waves are more energetic in the vicinity of submarine canyons (Shepard *et al.*, 1974; Shea and Broenkow, 1982). Observations at Del Mar and Mission Beach, far from canyons, do not support the idea that large internal tidal bores are a mere canyon effect. Another study on the geographical range of large internal tidal bores (Pineda, 1993) suggests that they are widespread.

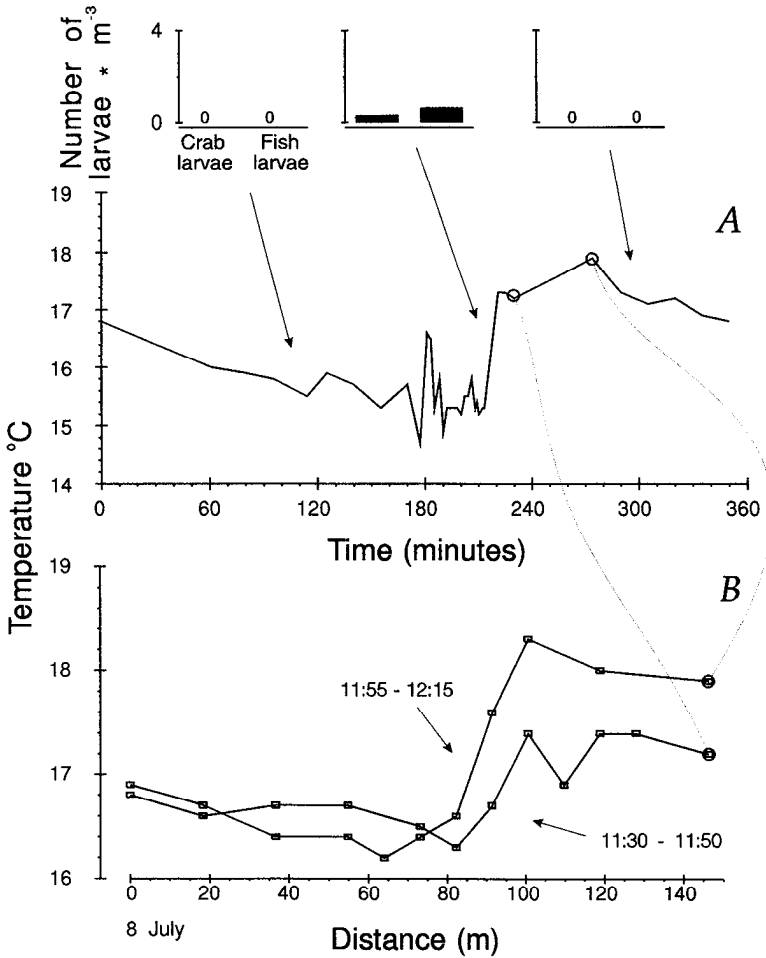


Figure 16. Neustonic larva abundance, surface-water-temperature time-series, (A) and surface-water-temperature transects (B) at Scripps Pier on 8 July 1992. Distance 0 m is closest to the surf zone. Distance 146 m is the same site where time-series observations (A) were made; the last observations in each of the transects are also observations in the time series. Times denote start and end of transects.

In Figure 1, it is assumed that the advective whole events are mostly two-dimensional. The extent of the front on June 28 suggests that at least on one occasion a two-dimensional assumption is justified. The model also assumes that the bodies of water remain relatively distinctive; of course, some mixing is to be expected. In particular, Figure 9A shows that the temperature of the warm-water body replacing the body advected by the first large-event bore is lower than pre-large-event temperature; this can be interpreted as cooling of the warm-water body (see also Fig. 1B in Pineda, 1991). Temperature records indicate that the bodies of water remain

distinctive. Minimal mixing during one of these events, inferred from thermocline structure, has previously been reported (Winant and Olson, 1976).

The observations reported here show that the seaward bottom currents are more energetic than the oncoming internal tidal bores. For observed seaward currents at Del Mar, high variance among different stages of phase two are obvious (Figs. 3–6). Calculated gravity current speeds and observed offshore speeds agree surprisingly well, however (Table 2). This result supports the interpretation that observed temperature and current fluctuations are gravity currents. Figures 3–6 show isotherms bending downward during phase two. This depression occurs immediately after the most energetic seaward bottom currents and could result from the momentum of the downslope gravity current as it enters subsurface, denser waters.

Arthur (1954) briefly described an event where “a narrow zone of debris, kelp, foam and jellyfish” was moving shoreward and that “the observed movement of debris may indicate a shoreward movement of warm, surface water.” Arthur proposed that temperature changes were due to the shoreward approach of a steep, or breaking leading edge of an internal wave trough. However, Arthur’s (1954) breaking-leading-edge conjecture does not explain the initial drop in surface water temperature. The shoreward movement of debris observed by Arthur (1954) has also been interpreted as evidence for the transport of larvae and debris by surface slicks generated by internal-waves (Shanks, 1983). Surface slicks, an epiphenomenon of internal waves (Ewing, 1950 a,b), would not explain the steep form of the wave nor the change in temperature described by Arthur. (This issue is further discussed below under “Onshore Transport of Neustonic Larvae.”)

While this contribution focuses on large internal tidal bores with lunar periodicity, small internal bores are ubiquitous in the summer (Cairns, 1967; Winant, 1974) and often occur daily for periods longer than 15 days at Scripps Pier in spring and summer (Fig. 1 in Pineda, 1991). Small events also appear to have an asymmetrical temperature trace and might produce some smaller-scale gravity flows.

a. Questions about scales. An important issue is the along-shore and cross-shore scale of large and small internal tidal bores and warm-water fronts. Along-shore coherence might be the result of either a single wave arriving at two different localities or of waves generated concurrently and arriving at different sites simultaneously. For along-shore scales, Arthur (1954) observed a single case of along-shore coherence at 4 km while temperature records at 40 km were not coherent. Lee (1961) observed short-period internal waves with alongshore coherence of 300 m; Summers and Emery (1963) observed nearly simultaneous arrival of crests of internal tidal waves at locations separated along-shore by 16 km in a deep-water location; Winant (1974) suggested that events observed at the Scripps Pier were mostly three-dimensional. Winant (1983) reported temperature and current coherence in Southern California for three frequency (*f*) bands. For the band that would include processes such as

diurnal breeze and surface and internal tides ($12 \text{ d}^{-1} > f > 1 \text{ d}^{-1}$), along-shore current coherence close to the surface was close to 0 at stations separated by more than 10 km. However, for along-shore current coherence close to the bottom, Winant found evidence of a propagating baroclinic tide. He pointed out that the cross-shelf internal tide could be a "localized response to the traveling longshore motion." The foam band at least 1 km long observed on 28 June 1990 suggests these events might have considerable along-shore scales.

For cross-shore scales, Cairns (1967) calculated a wavelength $\lambda = 9 \text{ km}$ for internal tides, and showed a single large internal tidal bore with a period at least 8 h. Even at very slow speeds, this would potentially yield cross-shore scales on the order of a few kilometers. Emery and Gunnerson (1973) reported λ averaging 9 km from cross-shore temperature transects. The Del Mar data set has been previously analyzed by Winant and Bratkovich (1981), but cross-shore spatial coherence was not reported in detail for the "tidal band" frequency ($6 \text{ d}^{-1} > f > 0.6 \text{ d}^{-1}$). For the higher frequency band ($f > 6 \text{ d}^{-1}$), phase speed of internal waves was 37 cm s^{-1} between the 60 and 30 m stations, and 22.7 cm s^{-1} between the 30 and 15 m stations. Results reported here show coherent currents at the 15, 30 and 60 m Del Mar stations (Figs. 3–6). For about 5–7 h during each event, bottom currents are directed onshore; at conservative current speeds (5 cm s^{-1}), a parcel of water could be transported 0.9–1.3 km in the cross-shore direction.

Data in Table 1 reveal that, at the 15 m depth station, the current and temperature scales are similar for the deepest sensor. For the shallowest instrument, the temperature time scale was twice the current scale. The scales of both the currents and the temperature close to the bottom are about half of the semidiurnal tide. These "double" frequency internal tides have been reported for other geographic regions and the details of origin are not known (Baines, 1986). Winant and Olson (1976) found that temperature and currents scales were similar for one event at Mission Beach.

b. Onshore transport of neustonic larvae. Physical transport mechanisms are critical to nearshore population and community ecology because adult population size is to some extent a function of the number of larvae that arrive at nearshore habitats and recruit successfully (Hatton, 1938; Coe, 1956; Yoshioka, 1982; Underwood and Denley, 1984; McConaugha, 1988; Roughgarden *et al.*, 1988). Given that different types of larvae may have dissimilar depth distributions, and that various transport mechanisms operate in distinct portions of the water column, it follows that different transport mechanisms should be invoked to explain the transport of larvae occupying dissimilar habitats within the water column. The work of Pineda (1991) supports that internal tidal bores are capable of transporting water-column larvae. Figures 12–16 support that neustonic larvae were being transported onshore by surface flow in concentrating fronts. While it is not explained why debris accumulate in the warm

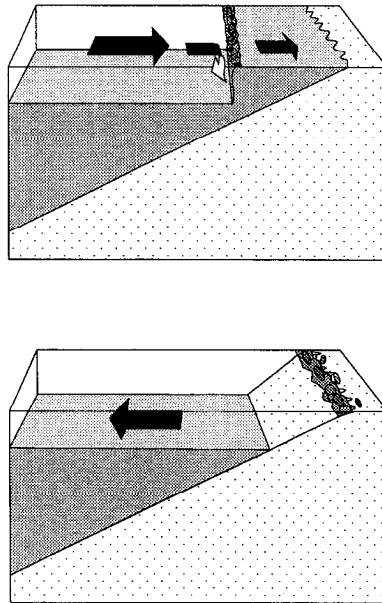


Figure 17. Schematic representation of the mechanism of delivery of debris and larvae to the shoreline by a warm-water front. The upper panel represents a shoreward moving warm-water front. The lower panel represents sinking of cold water after the delivery of the floating material to the shoreline. Arrows represent a conceivable pattern in the direction of the currents.

water front, it is inferred that a process of accumulation occurs from the observation that debris are concentrated at these fronts. Other phenomena that concentrate buoyant material such as Langmuir circulation or internal wave slicks do not explain the sharp horizontal surface temperature gradients.

Two mechanisms might help explaining the delivery of neustonic larvae by warm-water fronts to the shoreline. Figure 7 shows that over a period of 24 hours mean surface currents are directed onshore. This might result in a net onshore transport of material. Figure 17 illustrates a mechanism by which fronts might deliver the larvae to the shoreline. Visual observations of fronts in Figures 8, 10, 12–16 showed that they disappear at the shoreline, as the debris reach the surf zone. Once the debris encounter the surf zone, (Fig. 17, lower panel), the material might be taken over by the surf zone circulation, and/or deposited at the beach. The larvae could also respond behaviorally to the surf environment and initiate a settling response.

Shanks (1983) proposed an internal wave slick hypothesis to explain the onshore transport of neustonic larvae. There are several important differences between the mechanism proposed by Shanks and the one proposed here for explaining the onshore transport of neustonic larvae. In particular, Shanks (1983; 1986) invoked

unbroken internal waves as opposed to broken internal waves (e.g. internal bores) as the mechanism responsible for the transport of neustonic larvae. If surface slicks over unbroken internal waves could transport floating material, then this mechanism would also operate in deep water of the coastal or open ocean. This contrasts with the internal bore front mechanism which is essentially a shallow water, nearshore phenomenon. The surface-slick mechanism does not require advection of parcels of water, but advection of the kind presented in Figures 3–6 results from the bore-front mechanism. Shanks (1983; 1986) reasoned that slicks over unbroken internal waves were responsible for the transport of neustonic larvae because (a) larvae were neustonic (and then they could not be transported by internal bores, which would operate close to the bottom) and (b) peaks in larval transport did not occur during spring tides, when the largest internal waves would form internal bores. The first inference is contradicted by the results of this paper, which describes onshore transport of neustonic larvae by onshore-moving warm-water fronts, an epiphenomenon of large internal tidal bores. The second inference, that spring tides should produce the largest internal waves which in turn would produce internal bores is plausible. However, other scenarios are also plausible. For example, the largest internal waves produced in spring tides could break offshore, close to their site of generation, or dissipate before arriving close to the shoreline. Independent of any particular scenario, temperature data show that, on average, the largest internal tidal bores do not occur during spring tides at the Scripps Pier (Pineda, 1991) nor in other localities (Pineda, 1993). Therefore, the data do not support Shanks' (1983; 1986) second inference.

Evidence to support Shanks' hypothesis of shoreward transport of neustonic larvae by internal-wave generated surface slicks included lunar periodicity in larval crab settlement, position of the larvae in the surface, and onshore transport of drifters in two of five events. Lunar periodicity is better explained by the internal tidal bore hypothesis (Pineda, 1991) and the neustonic habitat of larvae is also well explained by the warm-water front hypothesis, as mentioned above. Surface slicks may look similar to onshore moving fronts (personal observation); measurements, such as surface temperature observations across convergent zones, are required to contrast the two phenomena. Furthermore, surface onshore flow obviously also occurs away from fronts (Figs. 3–6). It is possible that parcels of water being advected onshore could contain and carry surface slicks that might be separated from fronts. Thus, in the study of Shanks (1983) the actual identity of the mechanism responsible for the onshore transport of the drifters in the two events cannot be assessed unambiguously. Other surface-slick studies do not offer evidence that could contrast the warm-water-front with the surface-slick hypothesis (Jillett and Zeldis, 1985; Kingsford and Choat, 1986; Shanks and Wright, 1987; Shanks, 1986, 1988). See Le Fèvre and Bourget (1992) for further discussion contrasting the surface-slick and the internal-bore hypotheses.

While Shanks' (1983) mechanism is plausible, evidence for transport of floating particles by slicks is controversial. Ewing (1950b) concluded that internal-wave slicks propagate as a "wave of state," and that the surface film does not share its phase motion "but only its local oscillations." He pointed out that "dye or paper placed ahead of an advancing slick does not move along with it, but is overtaken, passed and left behind nearly in its original location." and that "sheets of paper . . . when placed in front of an on-coming slick, were observed to be drawn into the slick, and, after some minutes, to be ejected to the rear, indicating that the propagation of slicks does not depend directly on the surface flow." This is consistent with Zeldis and Jillett (1982) who found that juvenile galatheid crabs were linearly arranged by passing internal waves. While Ewing's experiments were done at sea, he cautioned that his conclusion rested chiefly on laboratory experiments. While Shanks (1983), Jillett and Zeldis, (1985) and Kingsford and Choat (1986) inferred that the mechanism was capable of transporting surface material from offshore waters to the nearshore, Ewing offered, to our best knowledge, the only direct experiments on the transporting capabilities of surface slicks. What is needed are more critical experiments to test the mechanism. Questions should center on the transporting capabilities of slicks and test for the transport of buoyant material for only a few minutes (as pointed by Ewing 1950b) or longer (as implied by Shanks 1983; Jillett and Zeldis, 1985; and Kingsford and Choat, 1986). Another question to answer experimentally is why only a few internal wave slicks would cause transport within the lunar cycle (Shanks, 1983). Consider the fact that "small event" internal tidal activity appears to occur daily at the Scripps Pier in summer and spring (Pineda, 1991; and unpubl. data). While these have associated slicks, peaks in invertebrate settlement do not occur daily. An additional issue to consider is that observations have shown high-frequency internal waves, and possibly accompanying slicks, following the head of internal bores (Cairns, 1967; Winant, 1974; Winant and Olson, 1976). Clearly, this does not refute the surface-slick hypothesis for the transport of neustonic larvae, and the surface-slick and internal-tidal bore hypotheses are not alternative. It is worth emphasizing, however, that temperature observations are needed when distinguishing different mechanisms for onshore transport in surface water by internal waves. If surface slicks do not require advection of parcels of water, then current data might also be required to unambiguously identify the slicks' transporting capabilities. These issues are important because different internal wave-mechanisms would have different transporting capabilities.

c. Some implications. Internal waves and bores have been observed in other geographic areas where they have been related to phenomena that might influence ecological systems: upwelling at the shelf break (Cooper, 1947, but see Cooper, 1952; Wolanski and Pickard, 1983; Sandstrom and Elliott, 1984; Pingree and Mardell, 1981; Mazé *et al.*, 1986; Serpette and Mazé, 1989), surface slicks (Ewing, 1950a,b),

advancing trains of surface waves, “tide rips” or breaking surface waves (Osborne and Burch, 1980; Apel *et al.*, 1985; Pingree and Mardell, 1985; Chapman *et al.*, 1991), and coastal seiching (Giese and Chapman, 1990).

Advection of the kind described in the sections above could play an important role in a number of nearshore systems. The understanding of such advection is clearly important for assessing the cross-shore transport of pollutants. Pollutants trapped in the nepheloid layer could be transported shoreward by events of the sort described here. Seaward flows close to the bottom in phase 2 at the 15, 30, and 60 m stations was detected with instruments at 12, 27 and 55 m (Figs. 3–6). These instruments cannot resolve a Stokes countercurrent between the bottom instruments and the seafloor. Nonetheless, neither high-resolution vertical temperature observations at the Scripps pier (with measurements at the seafloor; Winant, 1974) nor another recorded event (Winant and Olson, 1976) suggest the presence of the countercurrent. A Stokes counterflow might result in no net transport close to the bottom.

Energetic seaward bottom currents at the upper continental slope have been measured in other regions (e.g., Butman, 1988; Pingree and Le Cann, 1989). Some of these flows are baroclinic and occur at semidiurnal frequency. In particular, Butman describes 2 events where energetic seaward flows at “approximately semidiurnal periods” were correlated with variability in bottom water temperature at a similar-frequency (Butman, 1988; Fig. 5); these events appear very similar to those described here. Butman (1988) explained these fluctuations using an argument of vertical mixing in the bottom boundary layer. The hypothesis offered in this manuscript could be an alternative explanation to these phenomena.

As for many other cases of gravity currents (Simpson, 1987 for examples) it is likely that variability in topography could result in differential avenues for onshore and offshore flows. This issue could be important in selecting sewage-discharge locations. Because internal tidal bores are, on average, predictable within the lunar cycle, for pollutants lighter than sea-water, such as oil, it could be possible to plan cleaning efforts of hypothetical oil spills. The energetic along-shore (pers. obs.) and cross-shore currents near the surf zone might cause considerable erosion in shallow nearshore areas and might be important in estimating sand budgets. Furthermore, internal-tidal regimes vary in different nearshore areas (Pineda, unpublished), implying that different zones have different cross-shore transport regimes.

Shoreward advection of warm-water bodies might also be important for nearshore benthic and pelagic communities. Fronts accumulate material due to micro-circulation patterns, and are areas of intense biological dynamics (Le Fèvre, 1986 for a review). Other frontal systems have also been involved in larval transport phenomena (e.g. Epifanio, 1987; Kingsford, 1990; Farrell *et al.*, 1991; Graham *et al.*, 1992). Moreover, fronts might influence the development and transport of red tides. Two red-tide events associated with warm-water fronts in early 1990 (pers. obs.) were observed. Although the present work is focused on larvae at the surface, warm-water

fronts are obviously not restricted to the top surface layers. Occasional unquantified cod-end net sampling below the surface expression of the fronts showed very high abundance of zooplankters, including barnacle, bryozoan and gastropod larvae. The surface samples also included a unique community of organisms associated with the floating kelp (Pineda, unpubl.).

Acknowledgments. D. Checkley, P. Dayton, J. Enright, L. Haury, N. Holland, D. Schneider, and C. D. Winant critically read the manuscript. The comments of two anonymous reviewers were also helpful. The Scripps Institution of Oceanography supplied the water-column temperature data. C. D. Winant suggested the use and generously provided the Del Mar data and Denise Hagen kindly provided her serendipitous surface temperature data in Figure 8 B. Erika Del Castillo helped with moral and practical support throughout this study. M. Hendershott and C. Winant provided valuable suggestions. The people of Mexico supported this research through a CONACyT graduate fellowship.

REFERENCES

- Apel, J. R., J. R. Holbrook, A. K. Liu and J. J. Tsai. 1985. The Sulu Sea internal soliton experiment. *J. Phys. Oceanogr.*, 15, 1625–1985.
- Arthur, R. S. 1954. Oscillations in sea temperature at Scripps and Oceanside piers. *Deep-Sea Res.*, 2, 129–148.
- Baines, P. G. 1986. Internal tides, internal waves, and near-inertial motions, in *Baroclinic Processes on Continental Shelves*, 3, C. N. K. Mooers, ed., American Geophysical Union, Washington, 19–31.
- Butman, B. 1988. Downslope Eulerian mean flow associated with high-frequency current fluctuations observed on the continental shelf and upper slope along northeastern United States continental margin: implications for sediment transport. *Cont. Shelf Res.*, 8, 811–840.
- Cairns, J. L. 1966. Depth and strength of the seasonal thermocline in shallow water off Southern California, in *Proc. 3rd. U.S. Navy Symp. Military Oceanogr.*, 2, 27–38.
- 1967. Asymmetry of internal tidal waves in shallow coastal waters. *J. Geophys. Res.*, 72, 3563–3565.
- Cairns, J. L. and E. E. LaFond. 1966. Periodic motions of the seasonal thermocline along the southern California coast. *J. Geophys. Res.*, 71, 3903–3915.
- Cairns, J. L. and K. W. Nelson. 1970. A description of the seasonal thermocline cycle in shallow coastal water. *J. Geophys. Res.*, 74, 1127–1131.
- Chapman, D. C., G. S. Giese, M. G. Collins, R. Encarnación and G. Jacinto. 1991. Evidence of internal swash associated with Sulu Sea solitary waves? *Cont. Shelf Res.*, 11, 591–599.
- Coe, W. R. 1956. Fluctuations in populations of littoral marine invertebrates. *J. Mar. Res.*, 15, 212–232.
- Cooper, L. H. N. 1947. Internal waves and upwelling of oceanic water from mid-depths on to a continental shelf. *Nature (Lond.)*, 159, 579–580.
- 1952. Processes of enrichment of surface water with nutrients due to strong winds blowing on to a continental slope. *J. Mar. Biol. Assoc. U. K.*, 30, 453–464.
- Denman, K. L. and T. H. Powell. 1984. Effects of physical processes on planktonic ecosystems in the coastal ocean. *Oceanogr. Mar. Biol. Ann. Rev.*, 22, 125–168.
- Emery, K. O. and C. G. Gunnerson. 1973. Internal swash and surf. *Proc. Natl. Acad. Sci. U.S.A.*, 70, 2379–2380.
- Epifanio, C. E. 1987. The role of tidal fronts in maintaining patches of brachyuran zoea in estuarine waters. *J. Crustacean Biol.*, 7, 513–517.

- Ewing, G. C. 1950a. Relation between band slicks at the surface and internal waves in the sea. *Science (Washington D.C.)*, *111*, 91–94.
- 1950b. Slicks, surface films and internal waves. *J. Mar. Res.*, *9*, 161–187.
- Farrell, T. M., D. Bracher and J. Roughgarden. 1991. Cross-shelf transport causes recruitment to intertidal populations in central California. *Limnol. Oceanogr.*, *36*, 279–288.
- Giese, H. H. and D. C. Chapman. 1990. Causation of large-amplitude seiches on the Caribbean coast of Puerto Rico. *J. Phys. Oceanogr.*, *20*, 1449–1458.
- Graham, W. M., J. G. Field and D. C. Potts. 1992. Persistent “upwelling shadows” and their influence on zooplankton distributions. *Mar. Biol. (Berl.)*, *114*, 561–570.
- Hatton, H. 1938. Essais de bionomie explicative sur quelques espèces intercotidales d’algues et d’animaux. *Annls. Inst. Océanogr. Monaco.*, *17*, 241–238.
- Hauray, L. R., M. B. Briscoe and M. H. Orr. 1979. Tidally generated internal wave packets in Massachusetts Bay. *Nature (Lond.)*, *278*, 312–317.
- Jillet, J. B. and J. R. Zeldis. 1985. Aerial observations of surface patchiness of a planktonic crustacean. *Bull. Mar. Sci.*, *37*, 609–619.
- Kingsford, M. J. 1990. Linear oceanographic features: a focus for research on recruitment processes. *Aust. J. Ecol.*, *15*, 391–401.
- Kingsford, M. J. and J. H. Choat. 1986. Influence of surface slicks on the distribution and onshore movements of small fish. *Mar. Biol. (Berl.)*, *91*, 161–171.
- LaFond, E. C. 1962. Internal waves, *in* *The Sea, I*, M. N. Hill, ed., John Wiley and Sons, New York, 731–751.
- Le Fèvre, J. 1986. Aspects of the biology of frontal systems. *Adv. Mar. Biol.*, *23*, 163–299.
- Le Fèvre, J. and E. Bourget. 1992. Hydrodynamics and behaviour: transport processes in marine invertebrate larvae. *Trends in Ecol. Evol.*, *7*, 288–289.
- Lee, O. S. 1961. Observations on internal waves in shallow water. *Limnol. Oceanogr.*, *6*, 312–321.
- Lentz, S. J. and C. D. Winant. 1979. Ocean station Del Mar current meter campaign 1978–1979 data report SIO Reference Series No. SIO 79-27. Scripps Institution of Oceanography, University of California.
- Mazé, R., Y. Camus and J. Y. Le Tareau. 1986. Formation des gradients thermiques à la surface de l’océan, au dessus d’un talus, par interaction entre les ondes internes et le mélange dû au vent. *J. Cons. Int. Expl. Mer*, *42*, 221–240.
- McConaughy, J. R. 1988. Export and reinvasion of larvae as regulators of estuarine decapod populations. *Am. Fish. Soc. Sym.*, *3*, 90–103.
- Mullin, M. M. 1986. Spatial and temporal scales and patterns, *in* *Plankton dynamics of the Southern California Bight*, E. R. W. Eppley, ed., Springer-Verlag, Berlin 216–273.
- O’Brien, M. and J. Chernoff. 1934. Model law for motion of salt water through fresh. *Trans. Amer. Soc. Civil Eng.*, *99*, 576–594.
- Osborne, A. R. and T. L. Burch. 1980. Internal solitons in the Adaman Sea. *Science (Washington D.C.)*, *208*, 451–460.
- Pineda, J. 1991. Predictable upwelling and the shoreward transport of planktonic larvae by internal tidal bores. *Science (Washington D.C.)*, *253*, 548–551.
- 1993. Hydrodynamic forcing on shallow water communities: physical effects and ecological consequences of internal tidal bores. Ph.D. thesis, University of California, San Diego. 158 pp.
- Pingree, R. D. and B. Le Cann. 1989. Celtic and Armorican slope and shelf residual currents. *Prog. Oceanogr.*, *23*, 303–338.
- Pingree, R. D. and G. T. Mardell. 1981. Slope turbulence, internal waves and phytoplankton growth at the Celtic Sea shelf-break. *Philos. Trans. R. Soc. Lond. A Math. Phys. Sci.*, *302*, 663–682.

- 1985. Solitary internal waves in the Celtic Sea. *Prog. Oceanogr.*, *14*, 431–441.
- Roughgarden, J., S. Gaines and H. Possingham. 1988. Recruitment dynamics in complex life cycles. *Science (Washington D.C.)*, *241*, 1460–1466.
- Sandstrom, H. and J. A. Elliot. 1984. Internal tide and solitons on the scotian shelf: a nutrient pump at work. *J. Geophys. Res.*, *89*, 6415–6426.
- Serpette, A. and R. Mazé. 1989. Internal tides in the Bay of Biscay: a two-dimensional model. *Cont. Shelf Res.*, *9*, 795–821.
- Shanks, A. L. 1983. Surface slicks associated with tidally forced internal waves may transport pelagic larvae of benthic invertebrates and fishes shoreward. *Mar. Ecol. Prog. Ser.*, *13*, 311–315.
- 1986. Tidal periodicity in the daily settlement of intertidal barnacle larvae and an hypothesized mechanism for the cross-shelf transport of cyprids. *Biol. Bull.*, *170*, 429–440.
- 1988. Further support for the hypothesis that internal waves can cause shoreward transport of larval invertebrates and fish. *U.S. Fish Wild. Serv. Fish. Bull.*, *86*, 703–714.
- Shanks, A. L. and W. G. Wright. 1987. Internal-wave mediated shoreward transport of cyprids, megalopae, and gammarids and correlated longshore differences in the settling rate of intertidal barnacles. *J. Exp. Mar. Biol. Ecol.*, *114*, 1–13.
- Shea, R. E. and W. W. Broenkow. 1982. The role of internal tides in the nutrient enrichment of Monterey bay, California. *Estuar. Coast. Shelf Sci.*, *15*, 57–66.
- Shepard, F. P., N. F. Marshall and P. A. McLoughlin. 1974. “Internal waves” advancing along submarine canyons. *Science (Washington D.C.)*, *183*, 195–198.
- Simpson, J. E. 1987. *Gravity Currents: In The Environment And The Laboratory*. John Wiley and Sons, New York, 244 pp.
- Stevenson, R. E. and D. S. Gorsline. 1956. A shoreward movement of cool subsurface water. *Trans. Amer. Geophys. Union*, *35*, 553–557.
- Summers, H. J. and K. O. Emery. 1963. Internal waves of tidal period off Southern California. *J. Geophys. Res.*, *68*, 827–839.
- Underwood, A. J. and E. J. Denley. 1984. Paradigms, explanation and generalizations in models for the structure of intertidal communities on rocky shores, *in Ecological Communities: Conceptual Issues and the Evidence*, D. R. Strong, D. Simberloff, L. G. Abele and A. B. Thistle, eds., Princeton University Press, Princeton, New Jersey, 151–180.
- Winant, C. D. 1974. Internal surges in coastal waters. *J. Geophys. Res.*, *79*, 4523–4526.
- 1983. Longshore coherence of currents on the Southern California shelf during the summer. *J. Phys. Oceanogr.*, *13*, 54–64.
- Winant, C. D. and A. Bratkovich. 1981. Temperature and currents in the southern California shelf: a description of the variability. *J. Phys. Oceanogr.*, *11*, 71–86.
- Winant, C. D. and J. R. Olson. 1976. The vertical structure of coastal currents. *Deep-Sea Res.*, *23*, 925–936.
- Wolanski, E. and G. L. Pickard. 1983. Upwelling by internal tides and Kelvin waves at the continental shelf break on the Great Barrier Reef. *Aust. J. Mar. Freshwater Res.*, *34*, 65–80.
- Yoshioka, P. M. 1982. Role of planktonic and benthic factors in the population dynamics of the bryozoan *Membranipora membranacea*. *Ecol.*, *63*, 457–468.
- Zeldis, J. R. and J. B. Jillett. 1982. Aggregation of pelagic *Munida gregaria* (Fabricius) (Decapoda, Anomura) by coastal fronts and internal waves. *J. Plankton Res.*, *4*, 839–857.